

This paper is published as part of a PCCP Themed Issue on:

[Interfacial Systems Chemistry: Out of the Vacuum, Through the Liquid, Into the Cell](#)

Guest Editors: Professor Armin Götzhäuser (Bielefeld) & Professor Christof Wöll (Karlsruhe)

Editorial

[Interfacial systems chemistry: out of the vacuum—through the liquid—into the cell](#)

Phys. Chem. Chem. Phys., 2010

DOI: [10.1039/c004746p](#)

Perspective

[The role of “inert” surface chemistry in marine biofouling prevention](#)

Axel Rosenhahn, Sören Schilp, Hans Jürgen Kreuzer and Michael Grunze, *Phys. Chem. Chem. Phys.*, 2010

DOI: [10.1039/c001968m](#)

Communication

[Self-assembled monolayers of polar molecules on Au\(111\) surfaces: distributing the dipoles](#)

David A. Egger, Ferdinand Rissner, Gerold M. Rangger, Oliver T. Hofmann, Lukas Wittwer, Georg Heimel and Egbert Zojer, *Phys. Chem. Chem. Phys.*, 2010

DOI: [10.1039/b924238b](#)

[Is there a Au–S bond dipole in self-assembled monolayers on gold?](#)

LinJun Wang, Gerold M. Rangger, ZhongYun Ma, QiKai Li, Zhigang Shuai, Egbert Zojer and Georg Heimel, *Phys. Chem. Chem. Phys.*, 2010

DOI: [10.1039/b924306m](#)

Papers

[Heterogeneous films of ordered CeO₂/Ni concentric nanostructures for fuel cell applications](#)

Chunjuan Zhang, Jessica Grandner, Ran Liu, Sang Bok Lee and Bryan W. Eichhorn, *Phys. Chem. Chem. Phys.*, 2010

DOI: [10.1039/b918587a](#)

[Synthesis and characterization of RuO₂/poly\(3,4-ethylenedioxythiophene\) composite nanotubes for supercapacitors](#)

Ran Liu, Jonathon Duay, Timothy Lane and Sang Bok Lee, *Phys. Chem. Chem. Phys.*, 2010

DOI: [10.1039/b918589p](#)

[Bending of purple membranes in dependence on the pH analyzed by AFM and single molecule force spectroscopy](#)

R.-P. Baumann, M. Schranz and N. Hampf, *Phys. Chem. Chem. Phys.*, 2010

DOI: [10.1039/b919729j](#)

[Bifunctional polyacrylamide based polymers for the specific binding of hexahistidine tagged proteins on gold surfaces](#)

Lucas B. Thompson, Nathan H. Mack and Ralph G. Nuzzo, *Phys. Chem. Chem. Phys.*, 2010

DOI: [10.1039/b920713a](#)

[Self-assembly of triazatriangulenium-based functional adlayers on Au\(111\) surfaces](#)

Sonja Kuhn, Belinda Baisch, Ulrich Jung, Torben Johannsen, Jens Kubitschke, Rainer Herges and Olaf Magnussen, *Phys. Chem. Chem. Phys.*, 2010

DOI: [10.1039/b922882a](#)

[Polymer confinement effects in aligned carbon nanotubes arrays](#)

Pitamber Mahanandia, Jörg J. Schneider, Marina Khanef, Bernd Stühn, Tiago P. Peixoto and Barbara Drossel, *Phys. Chem. Chem. Phys.*, 2010

DOI: [10.1039/b922906j](#)

[Single-stranded DNA adsorption on chiral molecule coated Au surface: a molecular dynamics study](#)

Haiqing Liang, Zhenyu Li and Jinlong Yang, *Phys. Chem. Chem. Phys.*, 2010

DOI: [10.1039/b923012b](#)

[Protein adsorption onto CF₃-terminated oligo\(ethylene glycol\) containing self-assembled monolayers \(SAMs\): the influence of ionic strength and electrostatic forces](#)

Nelly Bonnet, David O'Hagan and Georg Hähner, *Phys. Chem. Chem. Phys.*, 2010

DOI: [10.1039/b923065n](#)

[Relative stability of thiol and selenol based SAMs on Au\(111\) — exchange experiments](#)

Katarzyna Szelągowska-Kunstman, Piotr Cyganik, Bjorn Schüpbach and Andreas Terfort, *Phys. Chem. Chem. Phys.*, 2010

DOI: [10.1039/b923274p](#)

[Micron-sized \[6,6\]-phenyl C61 butyric acid methyl ester crystals grown by dip coating in solvent vapour atmosphere: interfaces for organic photovoltaics](#)

R. Dabirian, X. Feng, L. Ortolani, A. Liscio, V. Morandi, K. Müllen, P. Samori and V. Palermo, *Phys. Chem. Chem. Phys.*, 2010

DOI: [10.1039/b923496a](#)

[Self-assembly of L-glutamate based aromatic dendrons through the air/water interface: morphology, photodimerization and supramolecular chirality](#)

Pengfei Duan and Minghua Liu, *Phys. Chem. Chem. Phys.*, 2010

DOI: [10.1039/b923595g](#)

Self-assembled monolayers of benzylmercaptan and para-cyanobenzylmercaptan on gold: surface infrared spectroscopic characterization

K. Rajalingam, L. Hallmann, T. Strunskus, A. Bashir, C. Wöll and F. Tucek, *Phys. Chem. Chem. Phys.*, 2010

DOI: [10.1039/b923628g](https://doi.org/10.1039/b923628g)

The formation of nitrogen-containing functional groups on carbon nanotube surfaces: a quantitative XPS and TPD study

Shankhamala Kundu, Wei Xia, Wilma Busser, Michael Becker, Diedrich A. Schmidt, Martina Havenith and Martin Muhler, *Phys. Chem. Chem. Phys.*, 2010

DOI: [10.1039/b923651a](https://doi.org/10.1039/b923651a)

Geometric and electronic structure of Pd/4-aminothiophenol/Au(111) metal–molecule–metal contacts: a periodic DFT study

Jan Kučera and Axel Groß, *Phys. Chem. Chem. Phys.*, 2010

DOI: [10.1039/b923700c](https://doi.org/10.1039/b923700c)

Ultrathin conductive carbon nanomembranes as support films for structural analysis of biological specimens

Daniel Rhinow, Janet Vonck, Michael Schranz, Andre Beyer, Armin Götzhäuser and Norbert Hampp, *Phys. Chem. Chem. Phys.*, 2010

DOI: [10.1039/b923756a](https://doi.org/10.1039/b923756a)

Microstructured poly(2-oxazoline) bottle-brush brushes on nanocrystalline diamond

Naima A. Hutter, Andreas Reitingner, Ning Zhang, Marin Steenackers, Oliver A. Williams, Jose A. Garrido and Rainer Jordan, *Phys. Chem. Chem. Phys.*, 2010

DOI: [10.1039/b923789p](https://doi.org/10.1039/b923789p)

Model non-equilibrium molecular dynamics simulations of heat transfer from a hot gold surface to an alkylthiolate self-assembled monolayer

Yue Zhang, George L. Barnes, Tianying Yan and William L. Hase, *Phys. Chem. Chem. Phys.*, 2010

DOI: [10.1039/b923858c](https://doi.org/10.1039/b923858c)

Holey nanosheets by patterning with UV/ozone

Christoph T. Nottbohm, Sebastian Wiegmann, André Beyer and Armin Götzhäuser, *Phys. Chem. Chem. Phys.*, 2010

DOI: [10.1039/b923863h](https://doi.org/10.1039/b923863h)

Tuning the local frictional and electrostatic responses of nanostructured SrTiO₃—surfaces by self-assembled molecular monolayers

Markos Paradinas, Luis Garzón, Florencio Sánchez, Romain Bachelet, David B. Amabilino, Josep Fontcuberta and Carmen Ocal, *Phys. Chem. Chem. Phys.*, 2010

DOI: [10.1039/b924227a](https://doi.org/10.1039/b924227a)

Influence of OH groups on charge transport across organic–organic interfaces: a systematic approach employing an idealTM device

Zhi-Hong Wang, Daniel Käfer, Asif Bashir, Jan Götzen, Alexander Birkner, Gregor Witte and Christof Wöll, *Phys. Chem. Chem. Phys.*, 2010

DOI: [10.1039/b924230a](https://doi.org/10.1039/b924230a)

A combinatorial approach toward fabrication of surface-adsorbed metal nanoparticles for investigation of an enzyme reaction

H. Takei and T. Yamaguchi, *Phys. Chem. Chem. Phys.*, 2010

DOI: [10.1039/b924233n](https://doi.org/10.1039/b924233n)

Structural characterization of self-assembled monolayers of pyridine-terminated thiolates on gold

Jinxuan Liu, Björn Schüpbach, Asif Bashir, Osama Shekhah, Alexei Nefedov, Martin Kind, Andreas Terfort and Christof Wöll, *Phys. Chem. Chem. Phys.*, 2010

DOI: [10.1039/b924246p](https://doi.org/10.1039/b924246p)

Quantification of the adhesion strength of fibroblast cells on ethylene glycol terminated self-assembled monolayers by a microfluidic shear force assay

Christof Christophis, Michael Grunze and Axel Rosenhahn, *Phys. Chem. Chem. Phys.*, 2010

DOI: [10.1039/b924304f](https://doi.org/10.1039/b924304f)

Lipid coated mesoporous silica nanoparticles as photosensitive drug carriers

Yang Yang, Weixing Song, Anhe Wang, Pengli Zhu, Jinbo Fei and Junbai Li, *Phys. Chem. Chem. Phys.*, 2010

DOI: [10.1039/b924370d](https://doi.org/10.1039/b924370d)

On the electronic and geometrical structure of the trans- and cis-isomer of tetra-tert-butyl-azobenzene on Au(111)

Roland Schmidt, Sebastian Hagen, Daniel Brete, Robert Carley, Cornelius Gahl, Jadranka Dokić, Peter Saalfrank, Stefan Hecht, Petra Tegeder and Martin Weinelt, *Phys. Chem. Chem. Phys.*, 2010

DOI: [10.1039/b924409c](https://doi.org/10.1039/b924409c)

Oriented growth of the functionalized metal–organic framework CAU-1 on –OH- and –COOH-terminated self-assembled monolayers

Florian Hinterholzinger, Camilla Scherb, Tim Ahnfeldt, Norbert Stock and Thomas Bein, *Phys. Chem. Chem. Phys.*, 2010

DOI: [10.1039/b924657f](https://doi.org/10.1039/b924657f)

Interfacial coordination interactions studied on cobalt octaethylporphyrin and cobalt tetraphenylporphyrin monolayers on Au(111)

Yun Bai, Michael Sekita, Martin Schmid, Thomas Bischof, Hans-Peter Steinrück and J. Michael Gottfried, *Phys. Chem. Chem. Phys.*, 2010

DOI: [10.1039/b924974p](https://doi.org/10.1039/b924974p)

Probing adsorption and aggregation of insulin at a poly(acrylic acid) brush

Florian Evers, Christian Reichhart, Roland Steitz, Metin Tolan and Claus Czeslik, *Phys. Chem. Chem. Phys.*, 2010

DOI: [10.1039/b925134k](https://doi.org/10.1039/b925134k)

Nanocomposite microstructures with tunable mechanical and chemical properties

Sameh Tawfik, Xiaopei Deng, A. John Hart and Joerg Lahann, *Phys. Chem. Chem. Phys.*, 2010

DOI: [10.1039/c000304m](https://doi.org/10.1039/c000304m)

Is there a Au–S bond dipole in self-assembled monolayers on gold?†

LinJun Wang,^{ac} Gerold M. Ranggner,^b ZhongYun Ma,^c QiKai Li,^c Zhigang Shuai,^{*ac}
Egbert Zojer^{*b} and Georg Heimel^d

Received 18th November 2009, Accepted 8th February 2010

First published as an Advance Article on the web 24th February 2010

DOI: 10.1039/b924306m

Self-assembled monolayers (SAMs) of functionalized thiols are widely used in organic (opto)electronic devices to tune the work function, Φ , of noble-metal electrodes and, thereby, to optimize the barriers for charge-carrier injection. The achievable Φ values not only depend on the intrinsic molecular dipole moment of the thiols but, importantly, also on the bond dipole at the Au–S interface. Here, on the basis of extensive density-functional theory calculations, we clarify the ongoing controversy regarding the existence, the magnitude, and the nature of that bond dipole.

The work function, Φ , of a metal is defined as the energy difference between its Fermi level, E_F , and the energy of an electron at rest directly outside the metal surface, E_{vac} . Thus, to modify Φ by an amount $\Delta\Phi$, a SAM must introduce a potential energy step between metal and vacuum. To allow for the rational design of molecules that induce a desired $\Delta\Phi$, the latter is commonly split into two additive components. The first, ΔE_{vac} , arises from the molecular ad-layer only and the second, ΔE_{BD} , reflects the interfacial charge rearrangements upon molecule–metal bonding. Disregarding atomic-scale lateral inhomogeneities in the SAM, each potential energy step is linked to a corresponding plane-averaged charge (re)distribution, $\rho(z)$, via the Poisson equation,^{1–3}

$$\nabla^2 E(z) = \frac{e}{\epsilon_0} \rho(z) \quad (1)$$

where e denotes the (by definition positive) elementary charge and ϵ_0 the vacuum permittivity. As only a net dipole moment perpendicular to the surface leads to a non-vanishing ΔE , eqn (1) is commonly replaced by the heuristic Helmholtz equation, where the two contributions to $\Delta\Phi$ are regarded as arising from two laterally homogenous dipole layers.^{1–9}

$$\Delta\Phi = \Delta E_{\text{vac}} + \Delta E_{\text{BD}} = -\frac{en}{\epsilon_0} \left[\frac{|\mu| \cos(\beta)}{\epsilon_{\text{eff}}(n)} + \mu_{\text{BD}}(n) \right] \quad (2)$$

^a Department of Chemistry, Tsinghua University, 100084 Beijing, P.R. China. E-mail: zgshuai@tsinghua.edu.cn;

Fax: +86/10/6279-7689; Tel: +86/10/6279-7689

^b Institute of Solid State Physics, Graz University of Technology, Petersgasse 16, A-8010 Graz, Austria.

E-mail: egbert.zojer@tugraz.at; Fax: +43/(0)316/873-8466;

Tel: +43/(0)316/873-8475

^c Key Laboratory of Organic Solids, Beijing National Laboratory for Molecular Sciences (BNLMS), Institute of Chemistry, Chinese Academy of Sciences, 100190 Beijing, P.R. China

^d Institut für Physik, Humboldt-Universität zu Berlin, Newtonstr. 15, D-12489 Berlin, Germany

† Electronic supplementary information (ESI) available: Computational methodology and additional computational results on the properties of the free-standing molecular monolayers. See DOI: 10.1039/b924306m

Here, n denotes the molecular packing density, $|\mu|$ is the dipole moment of the free molecule, and β is the angle between the dipole axes of the molecules in the SAM and the surface normal. Generally, the depolarization factor ϵ_{eff} and the *bond dipole* at the Au–S interface, μ_{BD} , depend on the coverage in a non-trivial manner,¹⁰ but the same n (full coverage) is assumed for all SAMs considered here.

For many adsorbates, the conceptual partitioning of $\Delta\Phi$ into a purely molecular part (first term in eqn (2)) and a bonding-induced part (second term in eqn (2)) is unambiguously defined.² However, for SAMs formed by thiols, two different partitioning schemes appear in the literature. For the molecular contribution to $\Delta\Phi$, thiols (*i.e.*, R–SH species) are considered in the first^{1–5} and R–S• radical species in the second.^{6–9} These correspond to two conceptually different points of view,



where the first regards the bonding of the SAM to the metal as *replacing* S–H bonds with S–Au bonds and the second as *forming* new bonds between R–S• radicals and gold. Naturally, appreciably different molecular dipole moments are found for the saturated and the radical species and, consequently, by virtue of eqn (2), also different ΔE_{vac} values (see ESI†). As, however, the final situation is identical in both approaches, *i.e.*, a thiolate SAM on a gold surface (R–S–Au) with one given $\Delta\Phi$, eqn (2) implies that then also the bonding-induced contribution to the work-function modification, ΔE_{BD} , must differ between the two approaches. In density-functional theory (DFT) calculations, the latter is obtained by applying eqn (1) to the plane-averaged charge-density differences, ρ_{diff} , that are associated with the processes indicated in eqn (3).^{1–3,9}

$$\rho_{\text{diff}}^{\text{sat}} = \rho_{\text{sys}} - \rho_{\text{Au}} - (\rho_{\text{sat}} - \rho_{\text{H}}) \quad (4a)$$

$$\rho_{\text{diff}}^{\text{rad}} = \rho_{\text{sys}} - \rho_{\text{Au}} - \rho_{\text{rad}} \quad (4b)$$

Here, the subscripts sys, Au, rad, sat, and H refer to the entire metal/SAM system, the pristine metal, the free-standing molecular monolayer of radical and H-saturated species, and the layer of saturating H-atoms, respectively. Experimentally, ΔE_{BD} can be extracted from $\Delta\Phi$ measurements on a series of molecules with the aid of their calculated dipole moments and reasonable estimates for all other quantities in eqn (2).^{4–7}

Notably, DFT calculations pursuing the *saturated* approach have found values of $\Delta E_{\text{BD}} \approx -1.2$ eV for SAMs of biphenylthiols on Au(111),^{1–3} while negligible values (-0.01 – 0.08 eV)

have been reported for SAMs of alkylthiols following the radical scheme.⁹ Even more strikingly, experimental studies on thiols with an aromatic ring adjacent to the –SH group have reported a ΔE_{BD} of -0.85 eV when relying on μ values calculated for saturated molecules,⁵ while a ΔE_{BD} between $+0.6$ and $+1.0$ eV has been found using μ values calculated for radicals.⁶ Thus, the bond dipole of thiols on gold appears to depend not only on the chemical structure of the molecular backbone but, rather unsatisfactorily, also on the chosen partitioning scheme. It is the purpose of the latter, however, to permit correlating the chemical structure of the SAM-forming molecules with the achievable $\Delta\Phi$, thus allowing for the rational design of suitable molecules. Therefore, the question arises which of the two possibilities is better suited to provide a chemically and physically insightful picture of the relevant interfacial processes.

To elucidate this question, we performed slab-type DFT band-structure calculations for a series of functionalized thiols on Au(111) using VASP,¹¹ the internal-coordinate geometry optimizer GADGET,¹² and XCRYSDEN¹³ (for details see ESI†). As shown in Fig. 1a, each molecule is endowed with a strongly polar head-group substitution that either lowers Φ in the case of the electron-donating amino group (–NH₂) or increases Φ in the case of the electron-accepting cyano group (–CN);¹⁴ note that the total dipole moments of these molecules are composed of the contributions from the head groups on one side and from the thiol groups on the other side, the latter pointing roughly in the direction of the S–H bonds (*vide infra*). An in-depth analysis of the electronic properties of the molecules shown in Fig. 1a as well as the corresponding SAMs is provided in ref. 14. For the sake of comparability, the same rectangular $p(\sqrt{3} \times 3)$ unit cell containing two molecules is assumed for all monolayers (Fig. 1b). To individually access all components in eqn (4), separate calculations were performed on the corresponding sub-systems listed there.

As it appears more natural and chemically intuitive (in contrast to R–S• radicals, the –SH terminated molecules are readily accessible to experiment), the saturated scenario is discussed first. There, when setting up the system for the free-standing molecular monolayer in order to determine ΔE_{vac} in eqn (2) and ρ_{sat} in eqn (4a), one is faced with the choice of where to place the hydrogen atom relative to the sulfur (Fig. 1c). Two positions can be identified, where the hydrogen lies in the plane defined by the sulfur and the two nearest carbon atoms. As the S–C bond is inclined to the surface normal by $>17^\circ$ for all investigated molecules and the C–S–H bond angle is only $\sim 97^\circ$, this results in the hydrogens to lie above the plane of the sulfur atoms in position II (*i.e.*, farther away from where the metal surface will be located once bonding is established), and below the sulfur plane in position I. As ΔE_{BD} clearly should reflect the bonding of sulfur to gold, the latter position is obviously a better choice; one is primarily interested in the interfacial charge rearrangements between sulfur and gold and not in some spatial region within the molecular ad-layer, *i.e.*, where the saturating hydrogen atoms are located in position II (Fig. 1c). The ΔE_{BD} values obtained with the hydrogen at position I in the free-standing thiol layer are listed in Table 1. They are all negative and they reflect the local polarisability¹⁴ of the molecular backbone

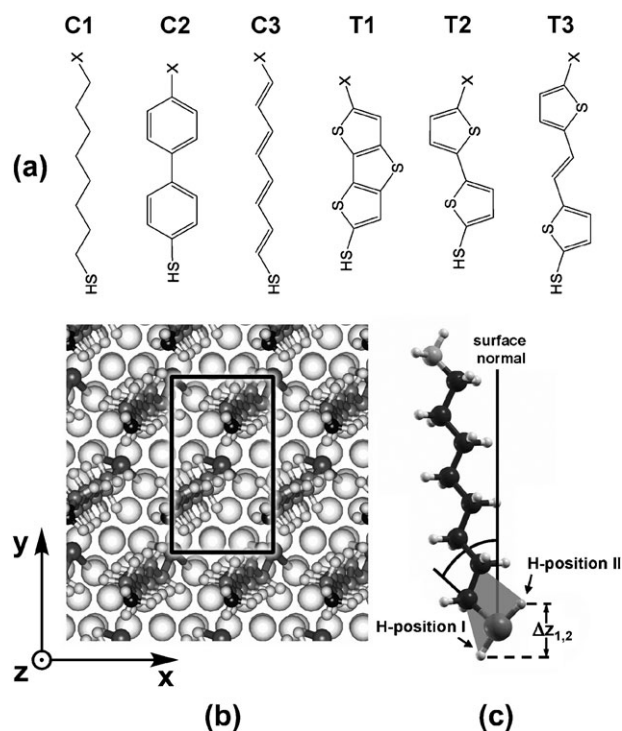


Fig. 1 (a) Chemical structures and labels of the investigated thiols; X stands for amino (–NH₂) and cyano (–CN) head-group substitutions. (b) Top view of the $p(\sqrt{3} \times 3)$ surface unit cell containing two molecules (shown for C1), which is assumed for all SAMs. (c) Side view of one NH₂-substituted C1 molecule in the free-standing H-saturated monolayer indicating the two possible hydrogen positions, the inclination of the S–C bond to the surface normal, and the height difference, $\Delta z_{1,2}$, between the two saturating hydrogen atoms in position I and II.

adjacent to the sulfur to some extent, *i.e.*, larger values are observed for more polarisable backbones.¹⁴ Notably, the value for the alkyl backbone C1 is non-zero. Also listed are the ΔE_{BD} values for hydrogen position II. Not only are they markedly different, but closer inspection of Table 1 reveals that the difference to the H-position I values increases essentially linearly with the height difference, $\Delta z_{1,2}$, between the hydrogens in the two positions (Fig. 1c), *i.e.*, with the projection of the local dipole moment around the –SH group onto the surface normal (*vide supra*); the corresponding plot is shown in Fig. 2.† This indicates that, using the saturated partitioning scheme, ΔE_{BD} also reflects the position of the saturating H-atoms and, thus, the orientation of the S–C bond and the molecular plane with respect to the surface normal (Fig. 1c).

To further test the ability of the saturated approach to provide chemically and physically insightful information, we also examined a different quantity, namely the “left-sided” ionisation potentials (IPs) of the free-standing saturated monolayers, which are defined as the energy difference between its highest occupied π -states (the highest fully delocalized σ -states in the case of C1)¹⁴ and E_{vac} on the thiol side;^{1–3} as the latter obviously differs from E_{vac} above the head-group substituents by ΔE_{vac} , also the “right-sided” IPs must differ from their left-sided counterparts by ΔE_{vac} .^{1–3} Again, the IP_{left} values in Table 1 reflect the chemical nature

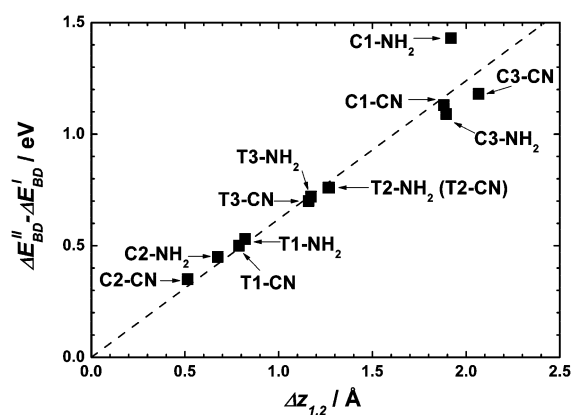


Fig. 2 Difference between the ΔE_{BD} values obtained with the saturated partitioning scheme for hydrogen positions I and II as a function of $\Delta z_{1,2}$, the height difference between the saturating hydrogen atoms in position I and II; † the dashed line is a linear fit through the origin.

Table 1 DFT-calculated vertical distance, $\Delta z_{1,2}$, between the saturating hydrogen atoms in positions I and II; † left-sided ionisation potential, IP_{left} , energy perturbation of the highest occupied delocalized orbitals upon metal–molecule bonding, E_{corr} , and potential energy step due to the bond dipole, ΔE_{BD} , for hydrogen position I as well as ΔE_{BD} for hydrogen position II obtained for the saturated partitioning scheme

System	H-Position				
	$\Delta z_{1,2}/\text{\AA}$	I IP_{left}/eV	I E_{corr}/eV	I $\Delta E_{BD}/\text{eV}$	II $\Delta E_{BD}/\text{eV}$
C1-NH ₂	1.919	7.74	0.03	-1.27	0.16
C1-CN	1.880	8.17	-0.01	-1.00	0.13
C2-NH ₂	0.675	5.03	0.14	-1.14	-0.69
C2-CN	0.515	5.13	0.17	-1.20	-0.85
C3-NH ₂	1.894	3.89	0.16	-1.87	-0.78
C3-CN	2.067	3.74	0.16	-2.06	-0.88
T1-NH ₂	0.821	4.26	0.14	-1.54	-1.01
T1-CN	0.788	4.30	0.14	-1.57	-1.07
T2-NH ₂	1.269	4.04	0.12	-1.70	-0.94
T2-CN	1.266	4.10	0.13	-1.71	-0.95
T3-NH ₂	1.173	3.99	0.13	-1.70	-0.98
T3-CN	1.160	4.01	0.13	-1.72	-1.02

of the molecular backbones, *i.e.*, lower values are found for structures with a more extended conjugation.¹⁴ Similarly to ΔE_{BD} , IP_{left} also reflects the orientation of the S–C bond or, more precisely, the projection of the local dipole moment of the –SH group onto the layer normal (see ESI†).

Finally, it has been observed that the right-sided IPs in the free-standing monolayers differ from the IP of the SAM bonded to the metal (reported in ref. 14) by a small amount, E_{corr} , which reflects the perturbation of the molecular electronic structure through metal–molecule bonding.^{1–3} As shown in Table 1, these E_{corr} values are below 0.2 eV for all investigated systems. This underlines that replacing the S–H bonds with S–Au bonds has little effect on the energy levels in the SAM and, again, the saturated partitioning scheme is seen to conserve the chemical information on the nature of the molecular backbone.

We now turn to the radical scenario where, instead of replacing S–H bonds with S–Au bonds, a new bond is formed between the R–S• species and the gold surface. While the radical is unlikely to actually participate in the process of

Table 2 DFT-calculated potential energy step due to the bond dipole, ΔE_{BD} , left-sided ionisation potential, IP_{left} , and energy perturbation of the highest occupied delocalized orbitals upon metal–molecule bonding, E_{corr} , obtained for the radical partitioning scheme

System	$\Delta E_{BD}/\text{eV}$	IP_{left}/eV	E_{corr}/eV
C1-NH ₂	-0.04	8.95	-0.02
C1-CN	-0.04	9.07	-0.09
C2-NH ₂	1.11	6.07	-1.11
C2-CN	0.96	6.08	-1.08
C3-NH ₂	1.33	6.11	-0.86
C3-CN	1.28	6.14	-0.83
T1-NH ₂	1.28	5.89	-1.11
T1-CN	1.19	5.88	-1.07
T2-NH ₂	1.22	5.81	-1.07
T2-CN	1.17	5.81	-1.08
T3-NH ₂	1.27	5.89	-0.99
T3-CN	1.23	5.89	-0.99

SAM formation, one obviously needs not be concerned with the position of a saturating hydrogen atom on the sulfur. The results obtained with the radical partitioning scheme are listed in Table 2. In agreement with previous studies following this approach,⁹ a vanishing ΔE_{BD} is found for the alkyl backbone C1 and, for all other molecular structures, ΔE_{BD} changes sign compared to the saturated scheme (Table 1); a potential dependence on the orientation of the S–C bond is hard to assess. Notably, the IP_{left} values in the radical case (Table 2) all lie within the narrow range of 5.8 – 6.1 eV (*cf.* ref. 8); the exception is again C1 due to the different nature (σ -orbital *vs.* π -orbital) of the highest occupied delocalized states.¹⁴ Additionally, the E_{corr} values are on the order of 1 eV, yet again with the exception of C1 (*vide infra*). This leads to the conclusions that, in the radical partitioning scheme, chemical information on the nature of the backbone is largely lost and that the electronic structure of the free-standing radical layer is significantly perturbed upon bonding to the metal.

The reason for these observations is that the radical character of the –S• termination dominates the electronic structure of the free-standing monolayer on the docking-group side and, consequently, also the interfacial charge redistributions upon metal–molecule bond formation. Removing the hydrogen from the sulfur in the thiol and, thus, converting the closed-shell molecule into a radical, induces major charge rearrangements on that side of the molecule. The latter can be expressed as $(\rho_{rad} + \rho_H) - \rho_{sat}$ and are shown in the left panels of Fig. 3. For all conjugated systems (C2 – T3), the charge redistributions resulting from hydrogen removal reach far onto the molecular backbones, as the sulfur is strongly coupled to their π -electron system. A qualitatively different behaviour is observed in the case of the alkylthiol (C1), where both the π -system and the radical character are strongly localized on the sulfur alone and, therefore, the delocalized σ -states are hardly affected by radical formation. When the bonds between radicals and gold are formed, *i.e.*, when charges are shifted according to eqn (4b), the molecule is essentially converted back to a closed-shell species and the aforementioned charge redistributions are largely reversed in the spatial region of the SAM (left panels in Fig. 3), but not quite. The actual chemical and physical information regarding the Au–S bonding lies hidden in the difference between the processes of removing the hydrogen atoms from the sulfur and “adding” the gold surface

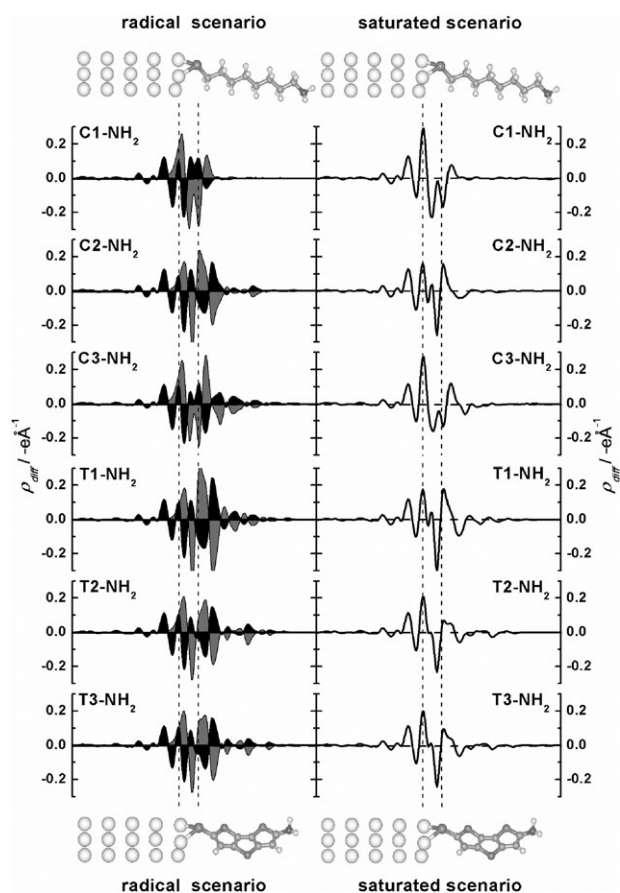


Fig. 3 Left panels: plane-integrated charge-density difference per unit-cell area, $(\rho_{\text{rad}} + \rho_{\text{H}}) - \rho_{\text{sat}}$, describing the removal of the hydrogen from the thiol (grey) and plane-integrated charge-density difference per unit-cell area, ρ_{diff} after eqn (4b), describing the bond formation between radical and metal (black). Right panels: plane-integrated charge-density difference per unit-cell area, ρ_{diff} after eqn (4a), describing the bonding of the hydrogen-saturated molecular monolayer to the metal. The curves in the right panels, which describe the actual bonding-induced interfacial charge rearrangements, are also the sum of the two curves in the left panel. The vertical lines indicate the (average) positions of the top-most gold layer and the sulfur atoms.

instead. Exactly this difference (right panels in Fig. 3), which actually corresponds to ρ_{diff} in the *saturated* partitioning scheme (eqn (4a)), is obscured in the radical approach.

To summarize, we have identified and discussed two distinctly different ways of defining the Au–S bond dipole in thiol SAMs on Au(111), the saturated and the radical scheme. With a well-defined choice for the positions of the saturating hydrogen atoms on the sulfur, the former conserves information on the chemical structure of the thiols, reflects the orientation of the S–C bond, and provides revealing insights

into the interfacial charge rearrangements that occur upon metal–molecule bonding. In particular, a considerable negative ΔE_{BD} is found for a wide range of molecules, including alkylthiols. On the other hand, when considering unsaturated R–S \cdot species as the origin of the molecular contribution to the work-function modification, chemical information on the SAM electronic structure is largely lost and the relevant bonding-related charge redistributions at the metal–molecule interface are not accessible, which clearly renders this second approach less appealing.

This work was supported by the Ministry of Science and Technology of China through the 973 program (Grants 2006CB806200 and 2006CB932100), by the FWF through project P20972-N20, and by the DFG through the Sfb448 “Mesoscopically Organized Composites”.

Notes and references

‡ As there are two inequivalent molecules per unit cell (Fig. 1b), the average $\Delta z_{1,2}$ values are reported.

- G. Heimel, L. Romaner, E. Zojer and J. L. Brédas, *Acc. Chem. Res.*, 2008, **41**, 721.
- G. Heimel, L. Romaner, E. Zojer and J. L. Brédas, *Nano Lett.*, 2007, **7**, 932.
- G. Heimel, L. Romaner, J. L. Brédas and E. Zojer, *Surf. Sci.*, 2006, **600**, 4548.
- B. de Boer, A. Hadipour, M. M. Mandoc, T. van Woudenberg and P. W. M. Blom, *Adv. Mater.*, 2005, **17**, 621.
- M. Malicki, Z. Guan, S. D. Ha, G. Heimel, S. Barlow, M. Rumi, A. Kahn and S. R. Marder, *Langmuir*, 2009, **25**, 7967.
- R. W. Zehner, B. F. Parsons, R. P. Hsung and L. R. Sita, *Langmuir*, 1999, **15**, 1121.
- I. H. Campbell, S. Rubin, T. A. Zawodzinski, J. D. Kress, R. L. Martin, D. L. Smith, N. N. Barashkov and J. P. Ferraris, *Phys. Rev. B: Condens. Matter*, 1996, **54**, 14321; I. H. Campbell, J. D. Kress, R. L. Martin, D. L. Smith, N. N. Barashkov and J. P. Ferraris, *Appl. Phys. Lett.*, 1997, **71**, 3528; D. M. Alloway, M. Hofmann, D. L. Smith, N. E. Gruhn, A. L. Graham, R. Colorado, V. H. Wysocki, T. R. Lee, P. A. Lee and N. R. Armstrong, *J. Phys. Chem. B*, 2003, **107**, 11690.
- Q. Sun and A. Selloni, *J. Phys. Chem. A*, 2006, **110**, 11396.
- P. C. Rusu and G. Brocks, *Phys. Rev. B: Condens. Matter Mater. Phys.*, 2006, **74**, 073414; P. C. Rusu and G. Brocks, *J. Phys. Chem. B*, 2006, **110**, 22628; V. De Renzi, R. Rousseau, D. Marchetto, R. Biagi, S. Scandolo and U. del Pennino, *Phys. Rev. Lett.*, 2005, **95**, 046804.
- L. Romaner, G. Heimel and E. Zojer, *Phys. Rev. B: Condens. Matter Mater. Phys.*, 2008, **77**, 045113; L. Romaner, G. Heimel, C. Ambrosch-Draxl and E. Zojer, *Adv. Funct. Mater.*, 2008, **18**, 3999.
- G. Kresse and J. Furthmüller, *Phys. Rev. B: Condens. Matter*, 1996, **54**, 11169; G. Kresse and J. Furthmüller, *Comput. Mater. Sci.*, 1996, **6**, 15; G. Kresse and D. Joubert, *Phys. Rev. B: Condens. Matter Mater. Phys.*, 1999, **59**, 1758.
- T. Bučko, J. Hafner and J. G. Angyan, *J. Chem. Phys.*, 2005, **122**, 124508.
- A. Kokalj, *Comput. Mater. Sci.*, 2003, **28**, 155. Code available from <http://www.xcrysden.org/>.
- L. J. Wang, G. M. Ranger, L. Romaner, G. Heimel, T. Bučko, Z. Y. Ma, Q. K. Li, Z. Shuai and E. Zojer, *Adv. Funct. Mater.*, 2009, **19**, 3766.